

1  
2  
3  
4  
5  
6  
7  
8  
9  
10  
11  
12  
13  
14  
15  
16  
17  
18  
19  
20  
21  
22  
23

*Revision 1*

### **Protolith carbon isotope ratios in cordierite from metamorphic and igneous rocks**

**William H. Peck**

Department of Geology, Colgate University, Hamilton, NY 13346, U.S.A.

#### **Abstract**

Cordierite commonly contain H<sub>2</sub>O and CO<sub>2</sub> in the channels formed by its ring structure. In many studies cordierite has been shown to have volatile contents and carbon isotope ratios consistent with high-temperature equilibrium, suggesting preservation of protolith carbon isotope ratios and motivating this survey of carbon isotopes in cordierite CO<sub>2</sub>. Cordierite CO<sub>2</sub> from pelitic country rocks in the Etive aureole have  $\delta^{13}\text{C}$  values of  $-20.70 \pm 1.27\text{‰}$  (n=10) that are unaffected by a ca. 150°C thermal gradient and fluid-saturated and undersaturated regimes. These  $\delta^{13}\text{C}$  values are consistent with expected carbon isotope ratios of organic carbon in protolith sediments. Similar lithologies from the Cooma and Huntly aureoles show more variable behavior in a more limited dataset, with some rocks preserving organic carbon  $\delta^{13}\text{C}$  values and others that may have been affected by externally-derived fluids. In cordierite-gedrite gneisses, carbon isotopes of cordierite (Crd) are distinct from those of cordierite in pelites; when excluding one outlier new data plus those from the literature average  $\delta^{13}\text{C}(\text{Crd}) = -12.51 \pm 2.45\text{‰}$  (n=17). These isotope ratios are higher than those of cordierite in typical metasedimentary protoliths, and are similar to published carbon isotope ratios of trace carbonate in altered submarine volcanic rocks, which are likely analogs for protoliths of many cordierite-gedrite rocks.

24 Igneous cordierite from granitic plutons have  $\delta^{13}\text{C} = -23.61 \pm 2.08\text{‰}$  (n=13), which is  
25 interpreted as reflecting a magmatic carbon budget dominated by organic carbon from  
26 sedimentary source rocks. In contrast, small pegmatites reported in the literature have  
27  $\delta^{13}\text{C}(\text{Crd}) = -10.20 \pm 3.06\text{‰}$  (n=6), which may indicate derivation from orthogneiss source  
28 materials. These new data show that carbon isotopes in cordierite can be used to help  
29 understand the protolith of even carbon-poor metamorphic rocks, and can also shed light  
30 on carbon in the sources of magmatic rocks. This latter approach has the potential for  
31 helping constrain the source rocks of peraluminous granitoids, which is controversial.  
32 Determining the extent to which organic carbon  $\delta^{13}\text{C}$  is preserved in granitoids is  
33 important for understanding the deep carbon cycle, and could serve as an important  
34 constraint in the search for low- $\delta^{13}\text{C}$  graphite inclusions in Hadean detrital zircons, which  
35 have been reported as a potential biosignature for the early Earth.

36

37

### Introduction

38 Cordierite ( $(\text{Mg,Fe})_2[\text{Al}_4\text{Si}_5\text{O}_{18}] \cdot (\text{H}_2\text{O}, \text{CO}_2)$ ) is a common mineral in low- to  
39 medium-pressure pelitic metamorphic rocks and is an accessory mineral in some  
40 peraluminous granitoids (Fig. 1). In addition to being an important petrologic indicator  
41 mineral, the composition of cordierite is also commonly used as an approach to constrain  
42 igneous and metamorphic fluids. The structural channels in cordierite have long been  
43 known to contain measurable volatile species, predominately  $\text{H}_2\text{O}$  and  $\text{CO}_2$ , and this  
44 property has been used as a tool by many workers for constraining the fluid chemistry of  
45 metamorphic and igneous rocks (e.g. Vry et al., 1990; Harley et al., 2002; Della Ventura  
46 et al., 2009; Rigby and Droop, 2008; 2011; Bebout et al., 2016). Cordierite from most of

47 these studies have H<sub>2</sub>O and CO<sub>2</sub> contents that are consistent with preservation of high-  
48 temperature fluid compositions, and cordierite from some localities show evidence for  
49 ‘leakage’ or re-equilibration during cooling and uplift.

50 Carbon isotope ratios of cordierite channel CO<sub>2</sub> have been measured in several  
51 studies (Armbruster et al., 1982; Vry et al., 1988; 1990; Vry and Brown 1992; Santosh et  
52 al., 1993; Fitzsimons and Matthey, 1995; Korja et al., 1996; Bebout et al., 2016), with the  
53 majority of the samples being from high-grade metamorphic rocks. For the most part  
54 these studies focused on fluid composition and constraining metamorphic fluid flow. In  
55 some cases evidence from carbon isotopes has been interpreted as indicating retrograde  
56 and channelized influx of a CO<sub>2</sub>-rich metamorphic fluid (Armbruster et al., 1982; Santosh  
57 et al., 1993). At other localities  $\delta^{13}\text{C}(\text{Crd})$  values are interpreted as indicating the  
58 possibility of mixing between protolith carbon and carbon from externally-derived fluid  
59 (Fitzsimons and Matthey, 1995). Carbon isotope heterogeneity at many localities is  
60 suggestive of a lack of mixing via a melt or a pervasive metamorphic fluid (Vry et al.,  
61 1988; 1990; Vry and Brown, 1992; Fitzsimons and Matthey, 1995). High-temperature  
62 isotopic equilibrium is also preserved between cordierite CO<sub>2</sub> and co-existing graphite  
63 (Vry et al., 1990; Fitzsimons and Matthey, 1995). Finally, variations in carbon isotopes of  
64 cordierite CO<sub>2</sub> from different localities in the Pikwitonei granulite domain (Superior  
65 Province, Canada) and Brattstrand Bluffs (East Antarctica) are suggestive preservation of  
66 pre-metamorphic protolith <sup>13</sup>C/<sup>12</sup>C (Vry and Brown, 1992; Fitzsimons and Matthey, 1995),  
67 which in part motivated this study.

68 This study focuses on testing the hypothesis of preservation of parent rock carbon  
69 isotope ratios in cordierite by examining several suites of well-constrained, genetically

70 related cordierite-bearing igneous and metamorphic rocks. The results confirm that, even  
71 in the absence of carbonate or graphite, often times cordierite faithfully preserves the  
72 carbon isotope ratio of metamorphic protoliths and igneous source materials, and thus  
73 gives us insights into the genesis of these rocks.

74

75

### **Materials and Methods**

76 Two sampling strategies were employed in this study. First, suites of igneous and  
77 metamorphic rocks were assembled that formed from parent rocks which typically have  
78 distinct carbon isotope ratios. These include S-type granitoids which are thought to  
79 originate from the melting of sediments (Chappell and White, 1992) and cordierite-  
80 gedrite gneisses and related rocks which are thought to be metamorphosed  
81 hydrothermally altered volcanic rocks (Peck and Smith, 2005). The metamorphic rocks  
82 analyzed for this study span a wide range of amphibolite to granulite facies temperatures  
83 (Fig. 1). Data from these samples are compared to carbon isotopes in cordierite from  
84 metamorphic rocks with clear sedimentary protoliths, which are well-represented in  
85 previous studies (Vry et al., 1990; Fitzsimons and Matthey, 1995; Korja et al., 1996;  
86 Bebout et al., 2016). The second sampling strategy was to examine two low-pressure  
87 contact-metamorphosed suites that had already been studied for H<sub>2</sub>O and CO<sub>2</sub> contents.  
88 Samples from the Etive aureole (Rigby et al., 2008) and the Huntly Complex (Droop et  
89 al., 2003; Rigby and Droop, 2008) allow the carbon isotopes of cordierite to be examined  
90 in similar pelitic lithologies that experienced conditions spanning several 100°C, and  
91 including partial melting (Fig. 1).

92           Samples were crushed, processed, and hand-picked using a binocular microscope  
93 to produce pure mineral separates. Cordierite was initially located using petrographic  
94 thin sections, followed by identification in matching rock billets. Because cordierite is  
95 visually so different in different rocks processing was tailored to individual samples.  
96 Some crushed samples were magnetically processed using a Frantz Isodynamic  
97 Separator, and for some rocks identification of cordierite in mineral separates was  
98 achieved with energy-dispersive X-ray spectroscopy using a scanning electron  
99 microscope with an Oxford X-max silicon drift X-ray detector. Alteration- and  
100 inclusion-free cordierite was the goal of mineral picking, and was achieved in some  
101 samples by scraping and breaking individual crystals using tweezers and dental tools. In  
102 very fine-grained hornfels samples inclusions could not be entirely avoided, and in some  
103 granitic samples it was impossible to entirely separate cordierite from pinitic alteration.  
104 Measured carbon contents thus may be minimum values due to the inclusion of non-  
105 cordierite material in the relatively large mineral separates needed for analysis. Several  
106 tests were done comparing inclusion-rich and altered mineral splits with pure mineral  
107 splits, which proved to have identical  $\delta^{13}\text{C}$  values within analytical uncertainty. All  
108 analyzed samples contain no visible graphite. A representative group of cordierite  
109 mineral splits were also soaked in cold 15% HCl, and showed visible evidence for  
110 dissolution after treatment. Partially dissolved samples have identical  $\delta^{13}\text{C}$  values to  
111 untreated samples, indicating a minimal role of carbonate alteration.

112           Powdered cordierite splits were combusted in a Costech ECS 4010 elemental  
113 analyzer (EA) online with a Delta Plus Advantage mass spectrometer in continuous flow  
114 mode after Peck and Tumpane (2007). Data are standardized to USGS-24 and instrument

115 conditions were monitored by multiple daily analyses of in-house standards, including a  
116 calcite that has been analyzed using phosphoric acid. Average cordierite sample size  
117 ranged from ca. 5–50 mg because of the variable and sometimes low carbon contents of  
118 cordierite, and the small analytical blank caused by trace carbon in the tin cups used for  
119 combustion (Peck and Tumpane, 2007). Reproducibility of cordierite samples averaged  
120  $\pm 0.12\%$  (81% of samples were duplicated or triplicated), which compares well to the  
121 average daily reproducibility of standards ( $\pm 0.05$ – $0.20\%$ ).

122

123

## Results

### 124 Contact-metamorphosed pelites

125 Cordierite from graphite-free pelitic metasediments was analyzed from the Etive  
126 contact aureole (Droop and Moazzen, 2007) and the Huntly complex, Scotland (Droop et  
127 al., 2003). Results are shown in Table 1 and figures 2 and 3. Samples of the Dalradian  
128 Leven Schist from Etive range from corundum to sillimanite metamorphic zones, and  
129 have very constrained  $\delta^{13}\text{C}(\text{cordierite}) = -22.18$  to  $-18.95\%$  ( $n=10$ ). Carbon contents  
130 range from 0.18–0.33 wt%  $\text{CO}_2$ . This similar but slightly higher than the 0.07–0.25 wt%  
131 range in  $\text{CO}_2$  concentrations measured using Fourier transform infrared spectroscopy  
132 (FTIR) spot analyses on these rocks by Rigby et al. (2008). These authors also  
133 documented systematic variability ( $\sim 0.1$  wt%  $\text{CO}_2$  in the middle aureole and  $\sim 0.2$  wt%  
134  $\text{CO}_2$  at the igneous contact) that is not seen in the new data, probably reflecting  
135 heterogeneity that is differently sampled while hand-picking 10s of milligrams for  
136 isotope analysis versus 15–20  $\mu\text{m}$  spot analyses by FTIR. At the Huntly complex three  
137 orthopyroxene-bearing hornfels samples have  $\delta^{13}\text{C}(\text{cordierite}) = -21.18$  to  $-17.97\%$ .

138 Carbon contents range from 0.12 to 0.37 wt% CO<sub>2</sub>. Three migmatitic rocks with igneous  
139 textures derived from Dalradian sediments have  $\delta^{13}\text{C}(\text{cordierite}) = -21.89$  to  $-15.07\%$ .  
140 Carbon contents for igneous-textured rocks are higher, and range from 0.41 to 0.49 wt%  
141 CO<sub>2</sub>. This difference was not seen in the narrower 0.08 to 0.17 wt% range in CO<sub>2</sub>  
142 concentrations measured from these rocks using FTIR by Rigby and Droop (2008).

143

#### 144 **Cordierite-gedrite gneisses**

145 Carbon isotopes were measured for cordierite-gedrite gneisses in eight samples  
146 from five well-characterized localities, all of which have been documented as having  
147 hydrothermally altered volcanic protoliths (Table 2; Fig. 2). Carbon isotope ratios for  
148 seven samples (four localities) span from  $-15.76$  to  $-9.25\%$  (average  $\delta^{13}\text{C} = -12.33\%$ ).  
149 One cordierite sample from the Spuhler Peak Metamorphic Suite (Tobacco Root  
150 Mountains, Wyoming Province) is  $-23.05\%$ . Carbon contents range from 0.12-2.38 wt%  
151 CO<sub>2</sub>. Vry et al. (1990) and Bebout et al. (2016) present data from cordierite-gedrite and  
152 related rocks that can be compared to new analyses. This includes analyses from two of  
153 the localities sampled in this study: the Manitouwadge and Orijärvi volcanogenic massive  
154 sulfide (VMS) camps, Superior Province and Svecofennian Orogen (Table 2). Literature  
155 values are very similar to the new analyses presented here: they have an average  
156  $\delta^{13}\text{C}(\text{Crd}) = -12.71\%$  and range from  $-16.50$  to  $-8.40\%$  (n=9).

157

#### 158 **Cordierite-bearing granitoids**

159 Cordierite was analyzed for carbon isotope ratio from 13 samples representing  
160 eight major intrusive complexes (Table 3). With the exception of the Cornucopia Stock

161 (Johnson et al., 1997) these samples are all from bodies thought to have formed at least in  
162 part by melting of sedimentary rocks (Chappell and White, 1992; Finger and Clemens,  
163 1995; Erdmann et al., 2004; Antunes et al., 2008). Carbon isotope ratios range from -  
164 27.05 to -20.07‰ (average  $\delta^{13}\text{C}(\text{crd}) = -23.61\text{‰}$ ). These carbon isotope ratios are  
165 distinctly different from the small cordierite-bearing pegmatites reported by Vry et al.  
166 (1990) and Bebout et al. (2016), which range from -14.0 to -6.9‰. Measured carbon  
167 contents of cordierite from granitoids range from 0.11-0.84 wt%  $\text{CO}_2$ . These are similar  
168 to the 0.03–0.62 wt% range in  $\text{CO}_2$  concentrations of four samples of cordierite-bearing  
169 granitoids analyzed by ion microprobe by Harley et al. (2002). Three samples related to  
170 cordierite granitoids were also analyzed. A mylonitic metasedimentary rock from the  
171 South Bohemian Batholith (Austria) has  $\delta^{13}\text{C}(\text{cordierite}) = -24.08\text{‰}$ . Two  
172 metasedimentary samples from the contact aureole around the Cooma granodiorite  
173 (Australia) have  $\delta^{13}\text{C}(\text{cordierite}) = -26.05$  and  $-12.41\text{‰}$ , while an sedimentary equivalent  
174 outside of the aureole has  $\delta^{13}\text{C}(\text{whole-rock}) = -30.80\text{‰}$  (Fig. 2).

175

## 176 Discussion

### 177 Cordierite channel volatiles during metamorphism

178 A number of studies have examined cordierite channel  $\text{H}_2\text{O}$  and  $\text{CO}_2$  in contact  
179 and regionally metamorphosed rocks. In some metamorphic rocks  $\text{H}_2\text{O}$  and  $\text{CO}_2$  contents  
180 are found to be consistent with fluid-saturation during peak metamorphic conditions, and  
181 in others low calculated  $a\text{H}_2\text{O}$  and  $a\text{CO}_2$  is taken as indicating fluid absence (e.g. Vry et  
182 al., 1988; Harley et al., 2002; Rigby and Droop, 2008). In most rocks  $\text{H}_2\text{O} \gg \text{CO}_2$   
183 contents, but in some localities  $\text{CO}_2 > \text{H}_2\text{O}$  contents (including  $\text{CO}_2 > 1$  wt%), in both



184 fluid saturated and fluid undersaturated rocks (Rigby and Droop, 2011). It has also been  
185 found that in some cases cordierites lose and/or re-equilibrate H<sub>2</sub>O (Harley et al., 2002;  
186 Rigby and Droop, 2008) or more rarely CO<sub>2</sub> (e.g. Rigby et al., 2008) after the peak of  
187 metamorphism, consistent with slower CO<sub>2</sub> diffusion rates than H<sub>2</sub>O in cordierite  
188 channels (Radica et al., 2016). The processes that regulate this ‘selective leakage’ are not  
189 well understood (Harley et al., 2002; Rigby and Droop, 2008).

190 Carbon isotope data from previous studies support the common retention of  
191 cordierite channel CO<sub>2</sub> after the peak of metamorphism (e.g. Vry et al., 1990; Santosh et  
192 al., 1993; Fitzsimons and Matthey, 1995), and also some cases where post-peak fluids  
193 have been recorded by cordierite channel  $\delta^{13}\text{C}$  values (Armbruster et al., 1982; Santosh et  
194 al., 1993). However, these studies did not focus on rocks where protolith  $\delta^{13}\text{C}$  was well  
195 constrained, or examine samples across a metamorphic gradient with a variable  
196 temperature and fluid regime. New data from the Etive aureole hornfelses shows  
197 incredibly consistent cordierite channel CO<sub>2</sub>  $\delta^{13}\text{C}$  values ( $-20.72 \pm 1.27\text{‰}$ , Fig 3),  
198 spanning from metamorphic temperatures of  $\sim 660^\circ\text{C}$  near the spinel-in isograd to  $\sim$   
199  $800^\circ\text{C}$  at the igneous contact (Droop and Moazzen, 2007). Over this temperature  
200 gradient metamorphic fluid compositions recorded by cordierite range from fluid-  
201 saturated with  $a_{\text{H}_2\text{O}} \approx 1$  far from the contact to fluid-undersaturated with  $a_{\text{H}_2\text{O}} \approx 0.5$  to 0.8  
202 at temperatures above the melt-in isograd (Rigby et al., 2008). Proximal ( $\leq 30$  m) to the  
203 igneous contact cordierite H<sub>2</sub>O and CO<sub>2</sub> contents are higher, perhaps due to magmatic  
204 fluid influx (Rigby et al., 2008). The one sample examined here that was shown by  
205 Rigby et al. (2008) to have these higher CO<sub>2</sub> contents is sample MM193Y, which has  
206  $\delta^{13}\text{C} = 21.09$  and 0.3 wt% CO<sub>2</sub>, indistinguishable from other samples in the aureole.

207 These data would suggest that there is negligible isotope fractionation of CO<sub>2</sub> in  
208 cordierite over these temperatures.

209 Measured  $\delta^{13}\text{C}$  values ( $-20.72 \pm 1.27\text{‰}$ ) are consistent with likely organic carbon  
210 in shale protoliths to the Leven Schist (e.g. Deines, 1980; Schidlowski, 2001). The  
211 Leven Schist does not contain graphite (Droop and Moazzen, 2007), but Neoproterozoic  
212 sediments correlative to the Dalradian Leven Schist elsewhere contain reduced carbon  
213 that has similarly low  $\delta^{13}\text{C}$  values, typically in the range of  $-28$  to  $-20\text{‰}$  (see Hayes et al.,  
214 1999). The initial carbon isotope ratio of reduced carbon would be expected to be  
215 fractionated during diagenesis and metamorphism, and bacterial processes and thermal  
216 decarboxylation typically shift  $\delta^{13}\text{C}$  values of the remaining carbon to higher values.  
217 These processes, in addition to variability in initial carbon isotope ratios, causes the  
218 variety of  $\delta^{13}\text{C}$  values found in sedimentary reduced carbon (Deines, 1980; Fig.  
219 2). Determining which processes operated at lower temperatures and to what extent is  
220 not always possible in high-grade metamorphic rocks, but the distribution of  $\delta^{13}\text{C}$  of  
221 kerogen and graphite in ancient rocks shows that the typical shift of reduced carbon  
222 during metamorphism of metasediments is on the order of a few per mil (Schidlowski,  
223 2001), and a similar result is seen here and in other studies of cordierite  $\delta^{13}\text{C}$ . Note that  
224 cordierite CO<sub>2</sub> originally from marine carbonate protoliths would have  $\delta^{13}\text{C} \approx 0\text{‰}$ , which  
225 is not observed in any cordierite analyzed in this study. If sample MM193Y was affected  
226 by CO<sub>2</sub>-rich late magmatic fluids then the  $\delta^{13}\text{C}$  of the fluid was likely initially acquired  
227 by the magma from country rock metasediments, but with no detectable isotopic  
228 fractionation during metamorphic devolatilization or magmatic degassing, so the  $\delta^{13}\text{C}$  of  
229 this sample has not changed. It is notable that these samples have identical  $\delta^{13}\text{C}(\text{Crd})$  in

230 fluid-undersaturated and fluid-saturated portions of the contact aureole, consistent with  
231 robust retention of protolith organic carbon  $\delta^{13}\text{C}$  values in cordierite channel  $\text{CO}_2$ .  
232 The six samples examined from the Huntly complex (Fig 2) are also cordierite-  
233 bearing and derived from Dalradian sediments; some are orthopyroxene-bearing  
234 hornfelses (black in Fig. 2) and others are igneous-textured diatexites (grey). Petrologic  
235 evidence points towards peak conditions of ca.  $900^\circ\text{C}$  and all samples having experienced  
236  $\sim 55\text{--}60\%$  melt extraction (Droop et al., 2003). Water contents of cordierite from these  
237 samples are interpreted as reflecting re-equilibration with melt during cooling after the  
238 peak of metamorphism, and more extensive exchange in diatexites which may have  
239 remained in contact with melt to lower temperatures than the hornfelses (Rigby and  
240 Droop, 2008). If this is the case, then more exchange with melt for diatexites than for  
241 hornfelses may explain the slightly higher  $\text{CO}_2$  contents measured in diatexite cordierite  
242 than measured in hornfels cordierite (Table 1). The cause of carbon isotope variability  
243 ( $\sim 3\text{‰}$  in hornfelses and  $\sim 7\text{‰}$  in diatexites) is less clear. Both lithologies have low  $\delta^{13}\text{C}$   
244 samples ca.  $-21$  to  $-22\text{‰}$ , similar to the Etive samples and consistent with  $\text{CO}_2$  derivation  
245 from sedimentary organic carbon (e.g. Deines, 1980; Schidlowski, 2001). The measured  
246 range in values could be interpreted as representing protolith rocks with a range in  $\delta^{13}\text{C}$   
247 values, or the variable effects of diagenesis, or mixtures of a sedimentary carbon  
248 signature with isotopically heavier  $\text{CO}_2$  from late magmatic fluids of the Huntly Gabbro.  
249 Mantle-derived carbon typically has  $\delta^{13}\text{C}$  values of  $-7$  to  $-5\text{‰}$  (Deines, 1980), and  
250 although carbon isotope fractionations between mafic melts (where carbon is mostly  
251 carbonate species) and  $\text{CO}_2$  are not well constrained for late magmatic temperatures,  $\text{CO}_2$   
252  $1\text{--}4\text{‰}$  heavier than a co-existing magma is consistent with experiments (Deines, 2004),

253 meaning that gabbro-derived CO<sub>2</sub> may explain a component of the carbon isotope  
254 variability in the Huntly samples. This kind of effect was not seen in the one Etive  
255 sample that may have experienced magmatic fluid alteration.

256         The other locality where multiple metamorphic samples were analyzed is the  
257 Cooma metamorphic complex, where Ordovician metasediments show progressive  
258 metamorphism up to melting in the aureole of the Cooma granodiorite (Chappell and  
259 White, 1976). Cordierite + andalusite + K-feldspar gneiss has  $\delta^{13}\text{C}(\text{Crd}) = -26.05\%$ ,  
260 similar to sedimentary organic carbon (e.g. Deines, 1980; Schidlowski, 2001) as does the  
261 whole-rock  $\delta^{13}\text{C} = -30.76\%$  for a shale sample from outside of the contact aureole (Table  
262 1). A lower  $\delta^{13}\text{C}$  of whole-rock reduced carbon than of cordierite channel CO<sub>2</sub> is  
263 consistent with the expected carbon isotope fractionation at metamorphic temperatures  
264 (Fig. 1). A migmatitic cordierite + sillimanite + K-feldspar gneiss from closer to the  
265 contact has  $\delta^{13}\text{C}(\text{Crd}) = -12.41\%$ . This anomalously high  $\delta^{13}\text{C}(\text{Crd})$  is accompanied by a  
266 higher  $\delta^{15}\text{N}(\text{whole-rock})$  compared to other aureole rocks, which Jia (2006) proposed  
267 could be caused by a magmatic fluid originating from the Cooma granodiorite.  
268 However, the Cooma granodiorite has  $\delta^{13}\text{C}(\text{Crd}) = -27.05\%$ , so the source of the high  
269  $\delta^{13}\text{C}$  (and likely  $\delta^{15}\text{N}$  as well) that affected the Cooma migmatite zone is likely not the  
270 Cooma granodiorite and is still unclear.

271         Of the three contact aureole case studies the Etive aureole has the most clear  
272 results: across variable temperature and fluid conditions during metamorphism  $\delta^{13}\text{C}(\text{Crd})$   
273 is unchanged. This may be in part because  $\delta^{13}\text{C}$  initially had a small range in the Leven  
274 Schist protolith sediments. The Huntly and Cooma complexes preserve protolith  
275 sedimentary  $\delta^{13}\text{C}(\text{Crd})$  values, but also higher  $\delta^{13}\text{C}$  values that may show the influence of

276 exotic fluids (which would be consistent with other geochemical evidence), or perhaps  
277 merely sedimentary variability in original  $\delta^{13}\text{C}$ . An inherent complication here is the  
278 large range in organic carbon  $\delta^{13}\text{C}$  in modern marine sediments: ca. -30 to -10‰,  
279 although most are in the range -27 to -20‰ (Deines, 1980). However, preservation of  
280 ‘typical’ organic carbon  $\delta^{13}\text{C}$  values in cordierite appears to be common in high-grade  
281 pelitic metasedimentary rocks, and has been documented in several studies (Vry et al.,  
282 1990; Santosh et al., 1993; Fitzsimons and Matthey, 1995; Korja et al., 1996; Bebout et al.,  
283 2016). Especially telling of the preservation of protolith  $\delta^{13}\text{C}$  are the very low  $\delta^{13}\text{C}$   
284 values of cordierite (and graphite) from Pikwitonei granulite domain (ca. -38 to -30‰),  
285 which likely is a reflection of the anomalously low  $\delta^{13}\text{C}$  carbon cycle excursion at ca. 2.7  
286 Ga known from lower-grade Archean rocks (Vry et al., 1988; 1990).

287

### 288 **Protoliths of cordierite-gedrite gneisses**

289         Although many cordierite-bearing gneisses have  $\delta^{13}\text{C}(\text{Crd})$  consistent with  
290 sedimentary organic carbon, others have higher  $\delta^{13}\text{C}$  values in the range -16.5 to -8.4‰  
291 (n= 9; Vry et al., 1990; Bebout et al., 2016). These samples are from cordierite-  
292 orthoamphibole (gedrite or anthophyllite) and related rocks, a group of schists or gneisses  
293 similar to metapelites but with unusually Ca-poor and Mg and Al-rich bulk compositions  
294 and typically lacking graphite. Some cordierite-gedrite localities have been ascribed to  
295 Mg-rich sedimentary rocks (e.g. Reinhardt, 1987) or metasediments that have been  
296 modified by melt extraction (e.g. Grant 1968), but the localities considered here have  
297 been shown to have hydrothermally altered volcanic protoliths (e.g. chlorite-sericite-  
298 quartz rocks). This is based on major and trace element geochemistry of these rocks

299 (Smith et al., 1992; Peck and Smith, 2005), their oxygen isotope ratios (Araujo et al.,  
300 1996; Peck and Valley, 2000; Burger et al., 2004), and their common association with  
301 VMS ore deposits (Araujo et al., 1996).

302 In addition to the ten published carbon isotope analyses of cordierite from  
303 cordierite-gedrite rocks in the literature, eight other rocks from well-characterized  
304 cordierite-gedrite gneiss localities were analyzed, including two from localities associated  
305 with VMS deposits that had already been sampled (Table 2). These rocks are from  
306 localities where major element geochemistry points to volcanic protoliths ranging from  
307 basalt to rhyolite in composition that have been variably leached of alkalis and calcium  
308 by seawater (Smith et al., 1992; Pan and Fleet, 1995; Blein et al., 2004; Burger et al.,  
309 2004, Peck and Smith, 2005). Oxygen isotopes from the Fishtail Lake and Bondy Gneiss  
310 Complex Grenville Province localities (Peck, 2000; Peck and Valley, 2000) and the  
311 Tobacco Root Mountains cordierite-gedrite rocks (Burger et al., 2004) indicate moderate  
312 to low-temperature hydrothermal alteration  $\leq$  ca. 250°C before high-grade  
313 metamorphism, while cordierite-gedrite rocks associated with the Manitouwadge VMS  
314 deposit have oxygen isotopes consistent with high temperature ( $\leq$  ca. 250°C) alteration  
315 (Araujo et al., 1996; Peck, 2000). These new samples all have  $\delta^{13}\text{C}(\text{Crd})$  values similar  
316 to those reported by Vry et al., (1990) and Bebout et al. (2016), except for one sample  
317 from the Tobacco Root Mountains with  $\delta^{13}\text{C}(\text{Crd}) = -23.05\text{‰}$ . In this sample cordierite is  
318 a texturally late replacement of garnet related to decompression (Fig. 1), where in the  
319 other samples cordierite more consistently shows textural equilibrium with other phases.  
320 Excluding this sample cordierite-gedrite gneisses have  $\delta^{13}\text{C}(\text{Crd}) = -12.51 \pm 2.45\text{‰}$  (n=17),  
321 considerably higher than the organic carbon signature in pelitic metasediments (Fig. 2).

322 A likely explanation for the measured  $\delta^{13}\text{C}(\text{Crd})$  values from cordierite-gedrite  
323 gneisses is that they record the carbon isotope ratio of the protolith, even though these  
324 rocks would normally be thought of as essentially carbon-free because of their general  
325 lack of carbonate or graphite. The departure from marine organic carbon  $\delta^{13}\text{C}$  values  
326 (Fig. 2) makes a clear distinction between cordierite-gedrite rocks and typical pelites. A  
327 possible modern analog for the protolith carbon source of cordierite-gedrite rocks is trace  
328 (<1%) carbonate found in altered seafloor basalts (Furnes et al., 2006). This trace  
329 carbonate is found in the bioaltered rims of pillow basalt from ocean crust with  
330 intermediate spreading rates, and typically has  $\delta^{13}\text{C}$  values between -15 and -5‰, which  
331 is attributed to derivation from  $\text{CO}_2$  generated by oxidation of organic material (Furnes et  
332 al., 2006). The average  $\delta^{13}\text{C}(\text{Crd})$  of cordierite-gedrite rocks ( $-12.51 \pm 2.45\text{‰}$ ) is  
333 essentially identical to the  $-12.08 \pm 2.90\text{‰}$  ( $n=12$ ) measured from trace carbon in basalts  
334 from the Costa Rica Rift (Furnes et al., 1999), and (with other geochemical data) fits well  
335 with a hydrothermally altered volcanic protolith. The carbon isotope ratios of cordierite-  
336 gedrite gneisses also help exclude some sources of protolith carbon. High  $\delta^{13}\text{C}$  values  
337 ( $>0\text{‰}$ ) caused by methanogenesis are found in altered volcanics from slow-spreading  
338 ocean crust (Furnes et al., 2006), which are inconsistent with carbon isotopes from  
339 cordierite-gedrite rocks. Likewise marine carbonate ( $\delta^{13}\text{C} \approx 0$ ) and mantle-derived carbon  
340 ( $\delta^{13}\text{C} \approx -7$  to  $-5\text{‰}$ ) are also excluded as a major contributors of carbon for these rocks.

341

#### 342 **Cordierite $\text{CO}_2$ in Granitoids**

343 In general, the carbon isotope systematics of magmatic carbon are not as well  
344 constrained as isotope systems that are hosted in refractory rock-forming igneous

345 minerals (e.g. U-Pb and O isotopes in zircon, Sm-Nd and O isotopes in garnet). In  
346 contrast, the carbon isotope budgets of magmas are mainly known from studies of  
347 magmatic volatiles (e.g. Blank and Brooker, 1994) and analysis of trace carbonate and  
348 reduced carbon in igneous rocks (Fuex and Baker, 1973; Hoefs, 1973). The magmatic  
349 volatile literature focuses on oceanic and subduction zone volcanism, so does not bear  
350 directly on the cordierite granites analyzed here. The interpretation of carbon isotopes of  
351 trace carbonate and reduced carbon in igneous rocks is problematic and controversial  
352 (Deines, 2004), and are likely prone to easy resetting by a variety of magmatic and late-  
353 stage hydrothermal processes, making this component of the deep carbon cycle difficult  
354 to constrain. In cordierite granites there is the unusual case of being able to sample CO<sub>2</sub>  
355 trapped in cordierite, a relatively refractory mineral, and to thus constrain carbon  
356 signatures in the igneous source materials.

357 Cordierite is a common accessory mineral in strongly peraluminous (mol Al<sub>2</sub>O<sub>3</sub>/  
358 Na<sub>2</sub>O+K<sub>2</sub>O+CaO > ~1.1) granitoids (Miller, 1985; Chappell and White, 1992). In some  
359 granites cordierite has been interpreted as being inherited from metasedimentary source  
360 rocks of the granites or entrained as xenocrysts from country rocks, but for the most part  
361 cordierite textures and mineral chemistry are consistent with being the result of formation  
362 from melt (Chappell et al., 1987; Clarke, 1995; Erdmann et al., 2005). The samples  
363 analyzed here (Table 3) range from small satellite plutons of larger batholiths (Cooma  
364 and Cornucopia) through major phases of batholiths occupying thousands of square  
365 kilometers (Kosciusko, South Mountain, South Bohemian Batholiths). Detailed  
366 petrologic studies of these plutons document a magmatic origin for cordierite in a variety  
367 of rock types, ranging from trondhjemite to granite in composition and including



368 cumulate and aplitic phases (Chappell and White, 1992; Finger and Clemens, 1995;  
369 Johnson et al., 1997; Erdman et al., 2005; Antunes et al., 2008).

370         Given the variety of magmatic cordierite analyzed it is surprising that carbon  
371 isotopes are so consistent:  $\delta^{13}\text{C}(\text{Crd}) = -23.61 \pm 2.08\%$  (n=13; Fig. 2). These values are  
372 exactly what would be expected for  $\text{CO}_2$  derived from organic carbon in sedimentary  
373 rocks (e.g. Deines, 1980; Schidlowski, 2001), but are distinct from other reservoirs such  
374 as mantle carbon and marine carbonate in limestones or marls. The  $\delta^{13}\text{C}(\text{Crd})$  is  
375 interpreted as reflecting the carbon isotope ratio of magmatic  $\text{CO}_2$  of the peraluminous  
376 granitic magmas, and a general similarity between carbon source materials among the  
377 studied plutons. In mafic magmas carbon is dissolved primarily as carbonate, so  
378 degassing of  $\text{CO}_2$  will fractionate  $\delta^{13}\text{C}$  (Blank and Brooker, 1994). Carbon in granitic  
379 magmas primarily exists as  $\text{CO}_2$ , so degassing will not appreciably fractionate  $\delta^{13}\text{C}$   
380 (Blank and Brooker, 1994; Dienes, 2004), and  $\delta^{13}\text{C}(\text{Crd})$  should closely reflect the  
381 isotope ratio of magmatic source materials.

382         Many peraluminous granitoids are interpreted to have formed from melting of  
383 sedimentary rocks at depth (e.g. S-type granites), but this interpretation is contested in  
384 some cases, and peraluminous compositions are also observed in rocks consistent with  
385 derivation from melting of igneous sources (Miller, 1985; Chappell and White, 1992). A  
386 review of the petrologic evidence for derivation from pelitic sediments versus psammic  
387 compositions or a mixture of sedimentary and igneous source rocks for strongly  
388 peraluminous granitoids is beyond the scope of this paper, but the magmatic carbon  
389 isotope ratios presented here help constrain some of these models. As a first-order  
390 interpretation the  $\delta^{13}\text{C}(\text{Crd}) = -23.61 \pm 2.08\%$  is consistent with organic carbon in clastic

391 metasedimentary rock as carbon source materials for the granites (e.g. shales or  
392 greywackes). Other metasedimentary rock-types have also been considered as possibly  
393 being important parental source materials to peraluminous granitoids, for example marls  
394 because of some similarities between the high CaO and Na<sub>2</sub>O of these rocks and  
395 Australian S-type granites (see Collins, 1996). The marine carbonate  $\delta^{13}\text{C} \approx 0\%$  of marls  
396 make them an unlikely source of carbon for cordierite granites.

397         The  $\delta^{13}\text{C}$  measured from cordierite can not easily be compared to the intermediate  
398 to felsic igneous source materials proposed as being parental to some peraluminous  
399 granitoids (e.g. Miller, 1985), as the bulk  $\delta^{13}\text{C}$  of this reservoir is not well constrained.  
400 Wedepohl (1995) estimates that the average carbon content of continental metamorphic  
401 rocks is ~800 ppm with  $\delta^{13}\text{C} = \text{ca. } -13\%$ , which does not match well the  
402 cordierite granitoids  $\delta^{13}\text{C}(\text{Cr}) = -23.61 \pm 2.08\%$ , but is a closer match to the  $\delta^{13}\text{C}(\text{Cr}) = -$   
403  $10.20 \pm 3.06\%$  (n=6) measured by Vry et al. (1990) and Bebout et al. (2016) for cordierite  
404 from small granite pegmatites. No cordierite-bearing pegmatites were sampled in this  
405 study, but this distinctive lithology appears to be commonly derived from melting of  
406 igneous source materials (Heinrich, 1950). At least some of these cordierite pegmatites  
407 are associated with cordierite-gedrite gneisses (e.g. Schumacher, 1990), which (as shown  
408 above) have a very similar  $\delta^{13}\text{C}(\text{Cr}) = -12.51 \pm 2.45\%$ .

409         The most straightforward interpretation of the bimodal distribution of igneous  
410 cordierite carbon isotope ratios is that the  $\delta^{13}\text{C}(\text{Cr}) = -10.20 \pm 3.06\%$  measured from  
411 cordierite pegmatites in other studies is indicative of orthogneiss or other igneous source  
412 materials, while the  $\delta^{13}\text{C}(\text{Cr}) = -23.61 \pm 2.08\%$  measured from the localities in Table 3  
413 represent organic carbon from pelitic paragneiss or other clastic metasediments. For

414 some plutons, such as Australian S-type granites, sedimentary rocks are generally agreed  
415 to be either the dominant (Chappell and White, 1992) or an important component in a  
416 mixture of the granite source materials (Kemp and Hawkesworth, 2004). In the latter  
417 model metasediment-derived melts would dominate the carbon budget of resulting  
418 magmas when mixing with mantle-derived melts, explaining the sedimentary  $\delta^{13}\text{C}$  of the  
419 cordierite granites. Substantial sediments in the source materials and in some cases  
420 assimilation of metasedimentary wall rocks are consistent with the petrologic  
421 characteristics of the other granitoid plutons sampled in this study (Finger and Clemens,  
422 1995; Erdman et al., 2005; Lackey et al., 2007; Antunes et al., 2008), save one body.  
423 Johnson et al. (1997) propose that the composition of the Cornucopia Stock is best  
424 explained by melting of mafic igneous lithologies in the lower crust. Excepting  
425 carbonatites, detailed carbon isotope studies of continental igneous rocks are few and far  
426 between (e.g. Duke and Rumble, 1986; Barnes et al., 2005), so there are clear open  
427 questions of the importance of source materials versus later processes such as  
428 assimilation or deuteric alteration on  $\delta^{13}\text{C}$  in granites. It may be in that in this case small  
429 amounts of metasedimentary rock in the source region dominate the carbon budget of the  
430 Cornucopia Stock magma but did not make a large impact on major or trace element  
431 geochemistry, or that low  $\delta^{13}\text{C}(\text{Crd})$  reflects late addition carbon from metasedimentary  
432 country rocks.

433         Carbon isotopes in evolved igneous rocks are in general poorly understood, partly  
434 because the low solubility of  $\text{CO}_2$  makes measurement of  $\delta^{13}\text{C}$  in magmatic volatiles  
435 from evolved rocks difficult (Blank and Brooker, 1994). This question is especially  
436 important because of the recent report of graphite with  $\delta^{13}\text{C} \approx -24\text{‰}$  included within a

437 single 4.1 Ga Jack Hills detrital zircon (Bell et al., 2015), which is interpreted by the  
438 authors as possibly being evidence for life on the earliest Earth. These Hadean detrital  
439 zircons are thought to derive from granitoids that had supracrustal lithologies as part of  
440 their source rocks (Peck et al., 2001; Bell et al., 2015), and the possibility that  $\geq 4.1$  Ga  
441 precursor rocks contained organic carbon has exciting implications for the evolution of  
442 life. Graphitized organic carbon inherited from clastic metasediments should on average  
443 have  $\delta^{13}\text{C} \approx -25\text{‰}$ , but graphite precipitated from magmatic  $\text{CO}_2$  could be measurably  
444 lower. The fractionation at  $900\text{--}700^\circ\text{C}$  between  $\text{CO}_2$  and graphite should be in the range  
445 of  $5\text{--}8\text{‰}$  (Deines and Eggler, 2009; Fig. 1), meaning that the cordierite granite  
446  $\delta^{13}\text{C}(\text{Crd}) \approx -24\text{‰}$  would be in equilibrium with  $\delta^{13}\text{C}(\text{graphite}) \approx -32$  to  $-29\text{‰}$ . More  
447 work remains to be done on the carbon isotope systematics of granitic magmas and the  
448 origin of reduced carbon in granitoids to better understand the graphite  $\delta^{13}\text{C}$  reported by  
449 Bell et al. (2015), and potential future graphite in Hadean zircons.

450

### 451 **Implications**

452 Carbon isotope studies have a clear role for understanding the deep carbon cycle,  
453 and isotope data is as often employed as a tool for understanding igneous and  
454 metamorphic source materials and subsequent rock alteration. Untangling these different  
455 isotopic signatures relies in part on identifying phases that preserve the part of the rock's  
456 history that is of interest and are resistant to subsequent processes. One approach is to  
457 focus on refractory minerals that have very high closure temperatures to diffusion as a  
458 way to 'see through' postmagmatic and metamorphic alteration, such as garnet and zircon  
459 (e.g. Peck et al., 2003; Lackey et al., 2011). This approach is difficult for carbon isotopes

460 in common igneous and meta-igneous rocks. Carbon dioxide is a minor component in  
461 magmas, and carbon is typically is present only in igneous rocks as trace carbonate and  
462 reduced carbon (Fuex and Baker, 1973; Hoefs, 1973). High-temperature graphite would  
463 meet the criteria of a refractory carbon-bearing phase, but is very rare in igneous rocks  
464 (Duke and Rumble, 1986).

465 Cordierite has been shown to be able to retain peak metamorphic or magmatic  
466 volatiles (Vry et al., 1990; Harley et al., 2002; Rigby and Droop, 2008), and thus allows  
467 carbon isotope analysis of trapped CO<sub>2</sub> even in rocks that do not contain another carbon-  
468 bearing mineral. Atmospheric pressure experiments of CO<sub>2</sub> diffusion rates in  
469 cordierite indicate relatively fast diffusion along channels, but the extent to which  
470 these experiments models geologic pressures and temperatures is unclear (Radica  
471 et al., 2016). Zoning in CO<sub>2</sub> concentrations in natural cordierite it has not been  
472 observed using FTIR (e.g. Rigby et al., 2008; Della Ventura et al., 2009), and the bulk  
473 cordierite  $\delta^{13}\text{C}$  data presented here and in previous studies point to relatively slow CO<sub>2</sub>  
474 diffusion. It has been proposed that alkali cations and CO<sub>2</sub> may occlude cordierite  
475 channels and retard volatile exchange (e.g. Vry et al., 1988), which might make alkali-  
476 rich igneous cordierites especially retentive of H<sub>2</sub>O and CO<sub>2</sub>. Zoning studies of CO<sub>2</sub> and  
477  $\delta^{13}\text{C}$  in cordierite-bearing rocks with different peak temperatures and cooling rates would  
478 be a welcome contribution to resolving some of these open questions and determining the  
479 effective closure temperature of carbon isotopes in cordierite. More work on the carbon  
480 isotope systematics of cordierite-bearing rocks would help better understand processes  
481 such as the carbon budgets of peraluminous granitic plutons and the bimodal distribution  
482 of  $\delta^{13}\text{C}(\text{Crd})$  from igneous rocks documented in this study. It will also serve as an

483 important benchmark in the search for further carbon isotope biomarkers in Hadean  
484 zircons (Bell et al., 2015).

485 High-temperature, refractory carbon-bearing phases are not common, but there  
486 has been success in analysis of carbonate in apatite (Peck and Tumpene, 2007) and  
487 scapolite (Moecher et al., 1994). This general approach might yield interesting  
488 information when applied to uncommon C-bearing minerals, for example silicate-  
489 carbonate minerals such as harkerite, spurrite, or tilleyite in high-temperature contact  
490 metamorphic rocks, or cancrinite in silica-undersaturated granitoids. The feldspathoids in  
491 general may be fruitful to investigate, as they have been shown to trap measurable CO<sub>2</sub> in  
492 channel and cage-like structures of their crystal lattices (Della Ventura et al., 2008).  
493 Reconnaissance analysis of beryl showed that the  $\delta^{13}\text{C}$  of channel CO<sub>2</sub> ranges from -25.8  
494 to 2.3‰ (n= 22), but does not clearly correlate with rock type or gemstone classification  
495 scheme (Peck and Dawson, 2015). This kind of variability may reflect an obstacle in  
496 interpreting the carbon isotope data from minerals with trace carbon, where there are not  
497 other phases present with which to assess isotope fractionation and the carbon budget of  
498 source rocks are not well constrained. A better understanding of how carbon isotopes are  
499 fractionated in metamorphic and especially igneous settings will allow a better  
500 understanding of the carbon budget of the crust and mantle.

501

## 502 **Acknowledgements**

503 In the early days of this project the late Bruce Chappell and Ian Williams very  
504 generously took me on a field trip to collect S-type granites in the Lachlan Fold Belt,  
505 which I gratefully acknowledge. I also thank Margarida Antunes, D. Barrie Clarke, Giles

506 Droop, Brent Elliott, Friedrich Finger, Kenneth Johnson, and Michael MacDonald for  
507 providing cordierite-bearing rocks for this study, as well as colleagues who donated  
508 samples that were not ultimately used. The use of samples that were analyzed for CO<sub>2</sub>  
509 and H<sub>2</sub>O contents using FTIR by Giles Droop and Martin Rigby is especially recognized.  
510 Simon Harley and John Valley are thanked for their thoughtful reviews, which improved  
511 the manuscript. Acquisition of the mass spectrometer at Colgate University was  
512 supported by NSF (EAR-0216179).

513

514

### References Cited

515 Antunes, I.M.H.R., Neiva, A.M.R., Silva, M.M.V.G. and Corfu, F. (2008) Geochemistry  
516 of S-type granitic rocks from the reversely zoned Castelo Branco Pluton (central  
517 Portugal). *Lithos*, 103, 445-465.

518 Araujo, S.M., Scott, S.D. and Longstaffe, F.J. (1996) Oxygen isotope composition of  
519 alteration zones of highly metamorphosed volcanogenic massive sulfide deposits; Geco,  
520 Canada, and Palmeiropolis, Brazil. *Economic Geology*, 91, 697-712.

521 Armbruster, T., Schreyer, W. and Hoefs, J. (1982) Very high CO<sub>2</sub> cordierite from  
522 Norwegian Lapland; mineralogy, petrology, and carbon isotopes. *Contributions to*  
523 *Mineralogy and Petrology*, 81, 262-267.

524 Barnes, C.G., Prestvik, T., Sundvoll, B. and Surratt, D. (2005) Pervasive assimilation of  
525 carbonate and silicate rocks in the Hortavaer igneous complex, north-central Norway.  
526 *Lithos*, 80, 179-199.

- 527 Bebout, G.E., Lazzeri, K.E., and Geiger, C.A. (2016) Pathways for nitrogen cycling in  
528 Earth's crust and upper mantle: A review and new results for microporous beryl and  
529 cordierite. *American Mineralogist*, 101, 7-24.
- 530 Blank, J.G. and Brooker, R.A. (1994) Experimental studies of carbon dioxide in silicate  
531 melts; solubility, speciation, and stable carbon isotope behavior. *Reviews in Mineralogy*,  
532 30, 157-186.
- 533 Blein, O., Corriveau, L. and Lafleche, M.R. (2004) Cordierite-orthopyroxene white  
534 gneiss; a key to unveiling premetamorphic hydrothermal activity in the Bondy gneiss  
535 complex, *in* Tollo, R.P., Corriveau, L., McLelland, J., and Bartholomew, M.J., eds.,  
536 *Proterozoic tectonic evolution of the Grenville orogen in North America*: Boulder,  
537 Colorado, Geological Society of America Memoir 197, p. 19-33.
- 538 Burger, H.R., Peck, W.H., Johnson, K.E., Tierney, K.A., Poulsen, C.J., Cady, P., Lowell,  
539 J., MacFarlane, W.A., Sincock, M.J., Archuleta, L.L., Pufall, A. and Cox, M.J. (2004)  
540 Geology and geochemistry of the Spuhler Peak Metamorphic Suite, *in* Brady, J.B.,  
541 Burger, H.R., Cheney, J.T., and Harms, T.A., eds., *Precambrian geology of the Tobacco*  
542 *Root Mountains, Montana*: Boulder, Colorado, Geological Society of America Special  
543 Paper 377, p. 47-70.
- 544 Chacko, T., Cole, D.R. and Horita, J. (2001) Equilibrium oxygen, hydrogen and carbon  
545 isotope fractionation factors applicable to geologic systems. *Reviews in Mineralogy and*  
546 *Geochemistry*, 43, 1-81.



- 547 Chappell, B.W. and White, A.J.R. (1992) I- and S-type granites in the Lachlan fold belt,  
548 in Brown, P.E. and Chappell, B.W., eds., *The Second Hutton Symposium on the Origin of*  
549 *Granites and Related Rocks*: Boulder, Colorado, Geological Society of America Special  
550 Paper 272, p. 1-26.
- 551 Chappell, B.W., White, A.J.R. and Wyborn, D. (1987) The importance of residual source  
552 material (restite) in granite petrogenesis. *Journal of Petrology*, 28, 1111-1138.
- 553 Clarke, D.B. (1995) Cordierite in felsic igneous rocks; a synthesis. *Mineralogical*  
554 *Magazine*, 59, 311-325.
- 555 Collins, W.J. (1996) Lachlan fold belt granitoids; products of three-component mixing. *In*  
556 Brown, M., Candela, P.A., Peck, D.L., Stephens, W.E. Walker, R.J., and Zen, E-A, eds.,  
557 *The Third Hutton Symposium on the Origin of Granites and Related Rocks*: Boulder,  
558 Colorado, Geological Society of America Special Paper 315, p. 171-181.
- 559 Deines, P. (1980) The isotopic composition of reduced organic carbon. *In* Fritz, A.P. and  
560 Fontes, J.C., eds., *Handbook of Environmental Isotope Geochemistry*, vol. 1, p. 329-406.
- 561 Deines, P. (2004) Carbon isotope effects in carbonate systems. *Geochimica et*  
562 *Cosmochimica Acta*, 68, 2659-2679.
- 563 Deines, P. and Eggler, D.H. (2009) Experimental determination of carbon isotope  
564 fractionation between CaCO<sub>3</sub> and graphite. *Geochimica et Cosmochimica Acta*, 73,  
565 7256-7274.

- 566 Della Ventura, G., Bellatreccia, F. and Piccinini, M. (2008) Channel CO<sub>2</sub> in  
567 feldspathoids: New data and new perspectives. *Rendiconti Lincei*, 19, 141-159.
- 568 Della Ventura, G., Bellatreccia, F., Cesare, B., Harley, S.L. and Piccinini, M. (2009)  
569 FTIR microspectroscopy and SIMS study of water-poor cordierite from El Hoyazo,  
570 Spain; application to mineral and melt devolatilization. *Lithos*, 113, 498-506.3
- 571 Droop, G.T.R., Clemens, J.D. and Dalrymple, D.J. (2003) Processes and conditions  
572 during contact anatexis, melt escape and restite formation; the Huntly Gabbro Complex,  
573 NE Scotland. *Journal of Petrology*, 44, 995-1029.
- 574 Droop, G.T.R. and Moazzen, M. (2007) Contact metamorphism and partial melting of  
575 Dalradian pelites and semipelites in the southern sector of the Etive Aureole. *Scottish*  
576 *Journal of Geology*, 43, Part 2, 155-179.
- 577 Duke, E.F. and Rumble, D. (1986) Textural and isotopic variations in graphite from  
578 plutonic rocks, south-central New Hampshire. *Contributions to Mineralogy and*  
579 *Petrology*, 93, 409-419.
- 580 Erdmann, S., Clarke, D.B. and MacDonald, M.A. (2004) Origin of chemically zoned and  
581 unzoned cordierites from the South Mountain and Musquodoboit batholiths, Nova Scotia,  
582 *in* Ishihara, S., Stephens, W.E., Harley, S.L., Arima, M. and Nakajima, T., eds., *The Fifth*  
583 *Hutton Symposium on the Origin of Granites and Related Rocks*: Boulder, Colorado,  
584 Geological Society of America Special Paper 389, p. 99-110.

- 585 Finger, F. and Clemens, J.D. (1995) Migmatization and 'secondary' granitic magmas;  
586 effects of emplacement and crystallization of 'primary' granitoids in southern Bohemia,  
587 Austria. *Contributions to Mineralogy and Petrology*, 120, 311-326.
- 588 Fitzsimons, I.C.W. and Matthey, D.P. (1995) Carbon isotope constraints on volatile  
589 mixing and melt transport in granulite-facies migmatites. *Earth and Planetary Science*  
590 *Letters*, 134, 319-328.
- 591 Fuex, A.N. and Baker, D.R. (1973) Stable carbon isotopes in selected granitic, mafic, and  
592 ultramafic igneous rocks. *Geochimica et Cosmochimica Acta*, 37, 2509-2521.
- 593 Furnes, H., Dilek, Y., Muehlenbachs, K. and Banerjee, N.R. (2006) Tectonic control of  
594 bioalteration in modern and ancient oceanic crust as evidenced by carbon isotopes. *Island*  
595 *Arc*, 15, 143-155.
- 596 Furnes, H., Muehlenbachs, K., Tumyr, O., Torsvik, T. and Thorseth, I.H. (1999) Depth of  
597 active bio-alteration in the ocean crust; Costa Rica Rift (Hole 504B). *Terra Nova*, 11,  
598 228-233.
- 599 Grant, J.A. (1968) Partial melting of common rocks as a possible source of cordierite-  
600 anthophyllite bearing assemblages. *American Journal of Science*, 266, 908-931.
- 601 Harley, S.L., Thompson, P., Hensen, B.J. and Buick, I.S. (2002) Cordierite as a sensor of  
602 fluid conditions in high-grade metamorphism and crustal anatexis. *Journal of*  
603 *Metamorphic Geology*, 20, 71-86.

- 604 Hayes, J.M., Strauss, H. and Kaufman, A.J. (1999) The abundance of  $^{13}\text{C}$  in marine  
605 organic matter and isotopic fractionation in the global biogeochemical cycle of carbon  
606 during the past 800 Ma. *Chemical Geology*, 161, 103-125.
- 607 Hoefs, J. (1973) Ein Beitrag zur Isotopengeochemie des Kohlenstoffs in magmatischen  
608 Gesteinen. *Contributions to Mineralogy and Petrology*, 41, 277-300.
- 609 Jia, Y. (2006) Nitrogen isotope fractionations during progressive metamorphism; a case  
610 study from the Paleozoic Cooma metasedimentary complex, southeastern Australia.  
611 *Geochimica et Cosmochimica Acta*, 70, 5201-5214.
- 612 Johnson, K., Barnes, C.G. and Miller, C.A. (1997) Petrology, geochemistry, and genesis  
613 of high-Al tonalite and trondhjemites of the Cornucopia Stock, Blue Mountains,  
614 northeastern Oregon. *Journal of Petrology*, 38, 1585-1611.
- 615 Kemp, A.I.S. and Hawkesworth, C.J. (2004) Granitic perspectives on the generation and  
616 secular evolution of the continental crust. *Treatise on geochemistry*. 3, 349-410.
- 617 Korja, T., Tuisku, P., Pernu, T. and Karhu, J. (1996) Field, petrophysical and carbon  
618 isotope studies on the Lapland granulite belt; implications for deep continental crust.  
619 *Terra Nova*, 8, 48-58.
- 620 Lackey, J.S., Erdmann, S., Hark, J.S., Nowak, R.M., Murray, K.E., Clarke, D.B. and  
621 Valley, J.W. (2011) Tracing garnet origins in granitoid rocks by oxygen isotope analysis;  
622 examples from the South Mountain Batholith, Nova Scotia. *Canadian Mineralogist*, 49,  
623 417-439.

- 624 MacDonald M.A. (2001) Geology of the South Mountain Batholith, Southwestern Nova  
625 Scotia. Nova Scotia Department of Natural Resources, Open File Report ME2001–  
626 22001, 281 pp.
- 627 MacDonald, M.A., and Clarke, D.B. (1985) The petrology, geochemistry, and economic  
628 potential of the Musquodoboit batholith, Nova Scotia. Canadian Journal of Earth  
629 Sciences, 22, 1633-1642.
- 630 Miller, C.F. (1985) Are strongly peraluminous magmas derived from pelitic sedimentary  
631 sources? Journal of Geology, 93, 673-689.
- 632 Moecher, D.P., Valley, J.W. and Essene, E.J. (1994) Extraction and carbon isotope  
633 analysis of CO<sub>2</sub> from scapolite in deep crustal granulites and xenoliths. Geochimica et  
634 Cosmochimica Acta, 58, 959-967.
- 635 Pan, Y. and Fleet, M.E. (1995) Geochemistry and origin of cordierite-orthoamphibole  
636 gneiss and associated rocks at an Archaean volcanogenic massive sulphide camp;  
637 Manitouwadge, Ontario, Canada. Precambrian Research, 74, 73-89.
- 638 Peck, W.H. and Dawson, T.L. (2015) Carbon isotope investigation of channel carbon  
639 dioxide in ring silicates: Cordierite and beryl. Geological Society of America Abstracts  
640 with Programs, 47(7), 762.
- 641 Peck, W.H. and Tumpene, K.P. (2007) Low carbon isotope ratios in apatite; an unreliable  
642 biomarker in igneous and metamorphic rocks. Chemical Geology, 245, 305-314.

- 643 Peck, W.H. and Smith, M.S. (2005) Cordierite-gedrite rocks from the Central  
644 Metasedimentary Belt boundary thrust zone (Grenville Province, Ontario);  
645 Mesoproterozoic metavolcanic rocks with affinities to the Composite Arc Belt. Canadian  
646 Journal of Earth Sciences, 42, 1815-1828.
- 647 Peck, W.H. and Valley, J.W. (2000) Genesis of cordierite-gedrite gneisses, Central  
648 Metasedimentary Belt boundary thrust zone, Grenville Province, Ontario, Canada.  
649 Canadian Mineralogist, 38, 511-524.
- 650 Peck, W.H., Valley, J.W., and Graham, C.M. (2003) Slow oxygen diffusion rates in  
651 igneous zircons from metamorphic rocks. American Mineralogist, 88, 1003-1014.
- 652 Peck, W.H., Valley, J.W., Wilde, S.A. and Graham, C.M. (2001) Oxygen isotope ratios  
653 and rare earth elements in 3.3 to 4.4 Ga zircons; ion microprobe evidence for high  $\delta^{18}\text{O}$   
654 continental crust and oceans in the early Archean. Geochimica et Cosmochimica Acta,  
655 65, 4215-4229.
- 656 Peck, W.H. (2000) Oxygen isotope studies of Grenville metamorphism and magmatism,  
657 United States. Ph. D. Thesis, University of Wisconsin (Madison, WI), 320 p.
- 658 Phillips, G.N., Wall, V.J. and Clemens, J.D. (1981) Petrology of the Strathbogie  
659 Batholith; a cordierite-bearing granite. Canadian Mineralogist, 19, 47-63.
- 660 Radica, F., Della Ventura, G., Bellatreccia, F., Cinque, G., Marcelli, A., and Guidi, M. C.  
661 (2016) The diffusion kinetics of  $\text{CO}_2$  in cordierite: an HT-FTIR microspectroscopy  
662 study. Contributions to Mineralogy and Petrology, 171, 1-13.

- 663 Reinhardt, J. (1987) Cordierite-anthophyllite rocks from North-west Queensland,  
664 Australia; metamorphosed magnesian pelites. *Journal of Metamorphic Geology*, 5, 451-  
665 472.
- 666 Rigby, M.J. and Droop, G.T.R. (2011) Fluid-absent melting versus CO<sub>2</sub> streaming during  
667 the formation of pelitic granulites; a review of insights from the cordierite fluid monitor,  
668 in van Reenen, D.D., Kramers, J.D., McCourt, S., and Perchuk, L.L., eds., *Origin and*  
669 *Evolution of Precambrian High-Grade Gneiss Terranes, with Special Emphasis on the*  
670 *Limpopo Complex of Southern Africa*: Boulder, Colorado, Geological Society of America  
671 Memoir 207, p. 39-60.
- 672 Rigby, M.J., Droop, G.T.R. and Bromiley, G.D. (2008) Variations in fluid activity across  
673 the Etive thermal aureole, Scotland; evidence from cordierite volatile contents. *Journal of*  
674 *Metamorphic Geology*, 26, 331-346.
- 675 Rigby, M.J. and Droop, G.T.R. (2008) The cordierite fluid monitor; case studies for and  
676 against its potential application. *European Journal of Mineralogy*, 20, 693-712.
- 677 Santosh, M., Jackson, D.H. and Harris, N.B.W. (1993) The significance of channel and  
678 fluid-inclusion CO<sub>2</sub> in cordierite; evidence from carbon isotopes. *Journal of Petrology*,  
679 34, 233-258.
- 680 Schidlowski, M. (2001) Carbon isotopes as biogeochemical recorders of life over 3.8 Ga  
681 of Earth history; evolution of a concept. *Precambrian Research*, 106, 117-134.

- 682 Schreyer, W. (1999) High-pressure experiments and the varying depths of rock  
683 metamorphism, in Craig, G.Y. and Hull, J.H., eds., *James Hutton – Present and Future*,  
684 Geological Society Special Publications 150, p. 59-74.
- 685 Schumacher, J.C. (1990) Reactions, textures, and mineral chemistry at the contact of a  
686 sillimanite-cordierite pegmatite and gedrite-cordierite gneiss from southwestern New  
687 Hampshire, USA. Geological Society of America Abstracts with Programs, 22, 125-125.
- 688 Smith, M.S., Dymek, R.F. and Schneiderman, J.S. (1992) Implications of trace element  
689 geochemistry for the origin of cordierite-orthoamphibole rocks from Orijarvi, SW  
690 Finland. *Journal of Geology*, 100, 545-559.
- 691 Vry, J., Brown, P.E., Valley, J.W. and Morrison, J. (1988) Constraints on granulite  
692 genesis from carbon isotope compositions of cordierite and graphite. *Nature*, 332, 66-68.
- 693 Vry, J.K. and Brown, P.E. (1992) Evidence for early fluid channelization, Pikwitonei  
694 granulite domain, Manitoba, Canada. *Canadian Journal of Earth Sciences*, 29, 1701-1716.
- 695 Vry, J.K., Brown, P.E. and Valley, J.W. (1990) Cordierite volatile content and the role of  
696 CO<sub>2</sub> in high-grade metamorphism. *American Mineralogist*, 75, 71-88.
- 697 Wedepohl, K.H. (1995) The composition of the continental crust. *Geochimica et*  
698 *Cosmochimica Acta*, 59, 1217-1232.
- 699



700 **Figure Captions**

701

702 **Figure 1.** Schematic pressure-temperature diagram and equilibrium carbon isotope  
703 fractionation ( $\Delta^{13}\text{C}$ ) between  $\text{CO}_2$  and graphite as a function of temperature. Sources of  
704 the peak temperatures for metamorphic rocks in this study are found Tables 1 and 2 (and  
705 references therein). Cordierite-gedrite gneiss localities: B= Bondy Gneiss Complex,  
706 F=Fishtail Lake, M=Manitouwadge, O= Orijärvi, and T= Tobacco Root Mountains  
707 (showing decompression path). Typical conditions for generation and emplacement of  
708 peraluminous granitoids are from Phillips et al. (1981), and the cordierite stability field is  
709 from Schreyer (1999). Carbon isotope fractionation from Deines and Eggler (2009) and  
710 Chacko (2001).

711

712 **Figure 2.** Carbon isotope analyses of cordierite (Crd) from analyzed samples (black and  
713 grey) and literature values (white; from Vry et al., 1990 and Bebout et al., 2016). Typical  
714 carbon isotopes of marine carbonate, mantle carbon, and organic carbon from recent  
715 marine sediments are from Deines (1980) and Schidlowski (2001), and altered basalt  
716 (Costa Rica Rift) is from Furnes et al. (1999). Grey range of marine organic carbon  
717 shows <10% of values; black shows >90% of values. Huntly Complex cordierite  
718 samples include hornfels (black) and igneous-textured metasediments (grey). ‘Other’  
719 samples from the Cooma contact aureole are 1: Shale from outside of the aureole (whole-  
720 rock analysis), 2: Cordierite + andalusite + K-feldspar gneiss, and 3: migmatitic  
721 cordierite + sillimanite + K-feldspar gneiss. Grey= mylonitic paragneiss, Bohemian  
722 Massif.

723

724

725 **Figure 3.** Carbon isotope ratios of cordierite in the pelitic Leven Schist from the high-  
726 temperature portion of the Etive thermal aureole. Metamorphic conditions of  
727 metasediments range from fluid saturated below the ~680°C melt-in isograd to strongly  
728 fluid-undersaturated above the ~705°C sillimanite-in isograd, and possibly affected by  
729 magmatic fluids at the ~800°C contact (Rigby et al., 2008). Carbon isotopes in cordierite  
730 are not influenced by variable metamorphic temperature or fluid regime. The spinel-in  
731 isograd is off of the diagram ca. 40 meters to the right.

732

733

734 Table 1. Carbon isotopes of cordierite from contact aureole pelitic rocks.

Sample		$\delta^{13}\text{C}$ (‰ PDB)	CO <sub>2</sub> (wt%)
<i>Etive aureole (Droop and Moazzen, 2007; Rigby et al., 2008)</i>			
MM193Y	Sillimanite zone hornfels (3m)	-21.09	0.31
MM197A	Sillimanite zone hornfels (15m)	-21.31	0.22
MM210A	Sillimanite zone hornfels (20m)	-20.79	0.29
MM166F	Sillimanite zone hornfels (90m)	-21.84	0.22
MM166A	Sillimanite zone hornfels (130 m)	-22.16	0.19
MM166H	Sillimanite zone hornfels (140m)	-19.15	0.19
MM169B	Sillimanite zone hornfels (140m)	-18.95	0.27
MM188B	Upper spinel zone hornfels (330 m)	-22.18	0.22
MM133	Lower spinel zone hornfels (450 m)	-19.02	0.33
MM185A	Lower spinel zone hornfels (490 m)	-20.76	0.24
<i>Huntly Complex (Droop et al., 2003; Rigby and Droop, 2008)</i>			
10035	Orthopyroxene-cordierite hornfels	-17.97	0.37
BQ41	Orthopyroxene- cordierite hornfels	-20.45	0.17
PIR1	Orthopyroxene- cordierite hornfels	-21.18	0.12
10038	Cordierite norite	-18.84	0.41
BQ38	Cordierite norite	-15.07	0.45
FOW1	Garnet-cordierite tonalite	-21.89	0.49

735 Note: Distance to the Etive igneous complex given parentheses. The upper and lower  
 736 spinel zones are separated by the melt-in isograd (Rigby et al., 2008).

737

738

739

740  
741  
742

743 Table 2. Carbon isotopes of cordierite from cordierite-gedrite gneisses.  
744

Sample	Lithology	Locality	$\delta^{13}\text{C}$ (‰ PDB)	$\text{CO}_2$ (wt%)	Reference
96FL6	Cordierite-gedrite gneiss	Fishtail Lake	-9.25	1.32	Peck and Valley, 2000
96FL7	Cordierite-gedrite gneiss	Fishtail Lake	-9.37	0.29	Peck and Valley, 2000
96FL11	Cordierite-biotite gneiss	Fishtail Lake	-13.45	2.38	Peck and Valley, 2000
96FL29	Cordierite-gedrite gneiss	Fishtail Lake	-12.61	0.40	Peck and Valley, 2000
97MW7	Cordierite-gedrite gneiss	Manitouwadge	-15.49	0.23	Peck, 2000
O-5B	Cordierite-gedrite gneiss	Orijärvi	-15.76	0.16	Smith et al., 1992
POD	Cordierite- kornrupine segregation	Bondy Gneiss Complex	-10.40	2.16	Peck, 2000
WP6B93	Cordierite-gedrite gneiss	Tobacco Root Mtns	-23.05	0.12	Burger et al., 2004

745

746

747

Table 3. Carbon isotopes of cordierite from cordierite-bearing granitoids.

Sample	Lithology and locality	$\delta^{13}\text{C}$ (‰ PDB)	$\text{CO}_2$ (wt%)	Reference
SMBCRD1	Aplite in Sandy Lake Monzogranite, SMB	-25.30	0.12	Macdonald , 2001
SMBCRD2	Harrietsfield Leucomonzogranite, SMB	-23.19	0.12	Macdonald , 2001
SMBCRD3	Aplite in Sandy Lake Monzogranite, SMB	-22.62	0.84	Macdonald , 2001
SMBCRD4	Harrietsfield Leucomonzogranite, SMB	-20.07	0.25	Macdonald , 2001
SMBCRD5	Harrietsfield Leucomonzogranite, SMB	-23.71	0.34	Macdonald , 2001
MBD15-438	Musquodoboit Batholith	-25.26	0.18	Macdonald and Clark, 1985
07AU14	Numbla Vale Monzogranite, Berridale Batholith	-21.74	0.11	Chappell and White, 1992
07AU15	Minnegans Monzogranite, Kosciusko Batholith	-25.00	0.40	Chappell and White, 1992
07AU27	Cooma Granodiorite, Murrumbidgee Batholith	-27.05	0.63	Chappell and White, 1992
G4	Granite, Castelo Branco Pluton, Iberian Variscan Belt	-26.49	0.59	Antunes et al., 2008
CS104	Trondhjemite, Cornucopia Stock	-22.38	0.66	Johnson et al., 1997
CS101	Trondhjemite, Cornucopia Stock Cordierite+garnet cumulate, Weinsberg granite, south	-22.75	0.76	Johnson et al., 1997
FI 77/85	Bohemian batholith	-21.37	0.41	Finger et al., 1997
FI 3/92	Mylonitic paragneiss, south Bohemian batholith	-24.08	0.49	Finger et al., 1997
07AU23	Andalusite+Kspar gneiss Cooma aureole	-26.05	0.81	Chappell and White, 1976
07AU26	Migmatite, Cooma aureole	-12.41	0.37	Chappell and White, 1976
07AU19	Shale, outside of Cooma aureole	-30.76	*	Chappell and White, 1976

748

Note: SMB= South Mountain Batholith. \* Whole-rock analysis

Figure 1

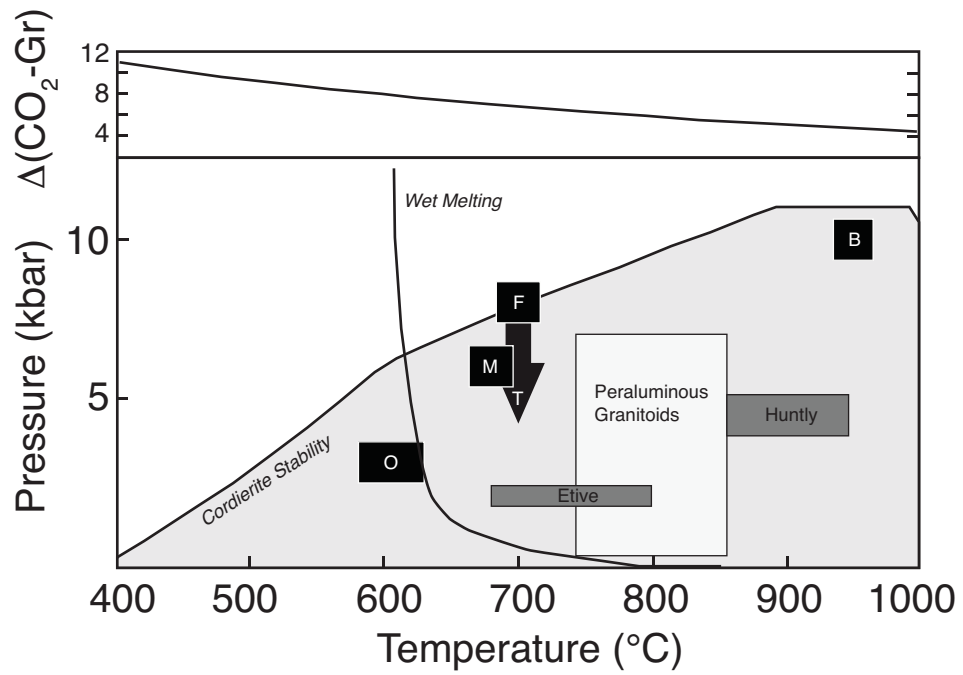


Figure 2

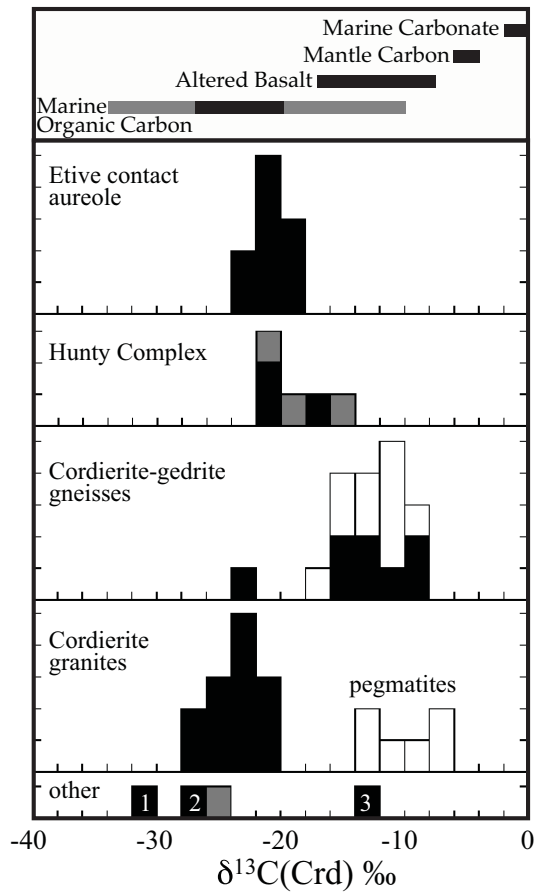


Figure 3

